Doppler-Tolerant Waveform Design and Signal Processing for Interference Immune Radar Systems

Robin Amar, Mohammad Alaee-Kerahroodi, Gabriel Beltrão, and Bhavani Shankar M. R.

***Abstract*—Dynamic targets in a radar system undergo a decrease in the matched filter gain as the Doppler tolerance limits for reliable operation are exceeded. In addition, interferers present in the field of view adversely effects the SINR of the victim sensor, thereby increasing false alarms. Features such as Doppler tolerance, uniqueness of the phase in every subpulse and subpulse processing architecture at the receiver are integrated together and a joint waveform and receiver design problem is discussed. An algorithm to devise unique waveforms is proposed which provides interference immunity to the transmit signal, improves compatibility of the system toward higher target velocities and provides optimal ISL/PSL metrics.**

***Index Terms*—Majorization-minimization, interference, polynomial phase.**

I. Introduction

Mutual Interference (MI) in radars is a challenge of high practical importance in Advanced driver assisted systems (ADAS) employed in modern vehicles [1]. This is due to the fact the radar sensors mounted on every vehicle operate in the shared unregulated frequency band and these transmissions are uncoordinated. This interference typically manifests as time-domain bursts which can result in diminished sensitivity [2].

Vehicular radar operation dominantly relies on the Frequency Modulated Continuous Wave (FMCW) technique with chirp sequence modulation in each Coherent Processing Interval (CPI). Every chirp uses Linear Frequency Modulation (LFM) waveform. It has two-fold advantages: Doppler tolerance and easy dechirp based receiver with low sampling requirements [3]. The reflected signal from dynamic targets with high relative velocity possess a Doppler shift which alters the return signal and deteriorates the Matched Filter (MF) gain. Because the LFM waveform is Doppler tolerant, the MF gain is less affected and the detection performance is preserved. In addition to the advantages, it has a serious drawback of lacking uniqueness. Transmitted chirp signal with LFM from a sensor (victim sensor) is prone to MI from another sensor (interferer) which possesses similar operating characteristics (such as chirp slope, bandwidth, etc.).

An alternative solution is transmitting noise waveform which is a form of random signal with arbitrary phase and amplitude. Keeping the amplitude fixed, it will be simplified to Phase Modulated Continuous Wave (PMCW) technique which possess uniqueness in phase and is therefore, impervious to MI [4]. In addition to these advantages, it has a disadvantage of Doppler intolerance. Although, loss in the MF response due to Doppler intolerance in Noise radars can be fairly dealt with the subpulse processing architecture in the receiver [5] but with longer pulse widths or fast moving targets the MF gain decrease. Due to dynamic targets, large Doppler shifts in noise radar systems cause detection loss in the MF output, which can be decreased by applying subpulse processing [5], [6]. However, if the intended speeds are too high or the pulse width is large, this strategy may not be enough to compensate the loss. In this paper, we have addressed this issue by integrating features such as Doppler tolerance, uniqueness of the phase in every subpulse and Integrated Sidelobe Level (ISL) minimization to synthesize a waveform [7] and utilize it with subpulse processing architecture at the receiver end [5].

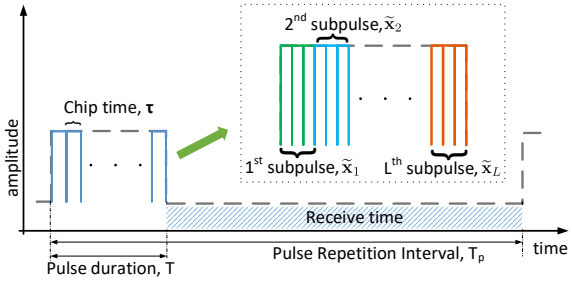

Fig. 1: Waveform time diagram

Recently, several studies have also considered the design of polyphase sequences with good Doppler tolerance properties [7]–[10]. In [11]–[13] ambiguity function shaping methods are used to obtain waveforms with low range sidelobes and high Doppler tolerance properties. Although, these approaches have addressed the problem in different ways, they have not been used in conjunction to solve the issue of sensing dynamic targets in the presence of interference.

Unlike previous studies, in this paper we propose an analytical approach for designing Doppler tolerant waveforms which are also immune to interference. Let $\mathbf{x} = [x_1, x_2, \cdots, x_N]^T \in \mathbb{C}^N$, denote the radar transmit waveform in the discrete form in *fast-time* domain. This waveform can be considered as the transmit sequence of a conventional noise radar, or a PMCW automotive radar, or even a pulsed radar equipped with the pulse compression technique during a single pulse of duration $T_c = N\tau$, where τ is the chip-duration. To improve the Signal to Noise Ratio (SNR), N_p such pulses are commonly transmitted in a single CPI with a time of T_{cp}. Fig. 1 depicts the timing diagram of the proposed radar waveform.

Assume a point target at range R approaching the radar system at a velocity of v. We consider ϵ as a complex term that

Robin Amar, SnT, University of Luxembourg, Luxembourg.
email: robin.amar@uni.lu
Mohammad Alaee-Kerahroodi, and Bhavani Shankar M. R. are with SnT, University of Luxembourg, Luxembourg.
Gabriel Beltrão is with IEE, Luxembourg.
This work was supported by FNR (Luxembourg) through the CORE project "SPRINGER: Signal Processing for Next Generation Radar" under grant C18/IS/12734677/SPRINGER.

indicates the backscattering effects of the target, channel fading, the gains and distortions introduced by the receiver Radio Frequency (RF) chain (assumed to be constant over a single Pulse Repetition Interval (PRI)). The received baseband signal reflected from this point target is sampled at Analog-to-Digital Converter (ADC) with a rate $f_s = \frac{1}{t_s} \approx \frac{1}{\tau}$. It is contaminated with the receiver noise and can be modeled as a noise vector $\mathbf{w} = [w_1, w_2, \cdots, w_N] \in \mathbb{C}^N$ where w_n is distributed normally with mean μ and variance σ^2 ($w_n \sim \mathcal{N}(\mu, \sigma^2)$). Thus, the resultant received signal is, $\mathbf{y} = \epsilon\mathbf{x} \odot \mathbf{p}(f_d) + \mathbf{w}$, where $\mathbf{p}(f_d)$ is Doppler steering vector defined in fast-time by, $\mathbf{p}(f_d) = [1, e^{j2\pi f_d t_s}, \cdots, e^{j2\pi f_d (N-1) t_s}]^T \in \mathbb{C}^N$. Now, we examine number of Doppler cycles observed in a single pulse duration [3] as $\zeta = f_d T_c$, where ζ indicates how many cycles of target Doppler appears in the fast-time duration[1]. Depending on the waveform type, if ζ is greater than a certain value [3], the Doppler shift can provide a mismatch loss at the output of the receiver, which can significantly reduce the detection capability.

To prevent this, a possible solution is to use Doppler-tolerant waveforms (chirp-like sequences [14]), which introduce range-Doppler coupling with lower loss in MF gain. The quadratic phase characteristic of chirp-like sequences causes MI, which reduces sensor reliability due to an increase in false targets or, in rare cases, receiver saturation. To avoid this, another idea is to design a transmit waveform that maintains its distinctiveness during the subpulse while being resilient to Doppler shift, which is considered in the sequel.

Notation: Boldface upper case letters denote matrices, boldface lower case letters denote column vectors, and italics denote scalars. $\mathbb{Z}$, $\mathbb{R}$ and $\mathbb{C}$ denote the integer, real and complex field, respectively. $\Re(\cdot)$ and $\Im(\cdot)$ denote the real and imaginary part respectively. $\arg(\cdot)$ denotes the phase of a complex number. The superscripts $(\cdot)^T$, $(\cdot)^*$, $(\cdot)^H$ and $(\cdot)^\dagger$ denote transpose, complex conjugate, conjugate transpose, and pseudo-inverse respectively. $X_{i,j}$ denotes the $(i,j)^{th}$ element of a matrix and x_i denotes the i^{th} element of vector $\mathbf{x}$. $\mathrm{Diag}(\boldsymbol{X})$ is a column vector consisting of all the diagonal elements of $\boldsymbol{X}$. $\mathrm{Diag}(\mathbf{x})$ is a diagonal matrix formed with $\mathbf{x}$ as its principal diagonal.

II. Problem Formulation

Let the transmit sequence $\mathbf{x}$ be partitioned into L subsequences each having length of M_l, where $l = 1, 2, \ldots, L$ such that every sub-sequence is considered a unique subpulse, say $\widetilde{\mathbf{x}}_l = [x_{\{1,l\}}, \cdots, x_{\{m,l\}}, \cdots, x_{\{M_l,l\}}]^T \in \mathbb{C}^{M_l}$, and it has a polynomial phase behavior, which can be expressed as $\arg(x_{\{m,l\}}) = \sum_{q=0}^{Q} a_{\{q,l\}} m^q$, where $m = 1, 2, \ldots, M_l$ and $a_{\{q,l\}}$ is the Q^{th} degree polynomial coefficient for the phase of the l-th sub-sequence with $q \in \{0, 1, 2, \ldots, Q\}$. The length of each subpulse M_l can be arbitrarily chosen which gives rise to the choice of any integer length N for the whole sequence, s.t. $\mathbf{x} = [\widetilde{\mathbf{x}}_1^T, \cdots, \widetilde{\mathbf{x}}_l^T, \cdots, \widetilde{\mathbf{x}}_L^T]^T \in \mathbb{C}^N$. The aperiodic autocorrelation of the transmitting waveform at lag k (e.g. MF output at the radar receiver) is defined as $r_k = \sum_{n=1}^{N-k} x_n x_{n+k}^* = r_{-k}^*, \quad k = 0, \ldots, N-1$. The transmit waveform must be good in terms of autocorrelation sidelobes in most radar applications. ISL, described mathematically as, ISL $\triangleq \sum_{\substack{k=-N+1 \\ k\neq 0}}^{N-1} |r_k|^2$, is a metric that quantifies the goodness of the transmit waveform [14]. Using the ISL as the objective function, we can formulate the optimization problem for designing subpulses in a sequence, where each subpulse has different characteristics in terms of subpulse length, instantaneous phase, and phase behavior (thus Doppler-tolerance property[2]). This problem can be stated as,

$$\mathcal{P}_1 \begin{cases} \underset{a_{\{q,l\}}}{\text{minimize}} & \displaystyle\sum_{k=1}^{N-1} |r_k|^2 \\ \text{subject to} & \arg(x_{\{m,l\}}) = \displaystyle\sum_{q=0}^{Q} a_{\{q,l\}} m^q, \\ & |x_{\{m,l\}}| = 1, \end{cases} \tag{1}$$

where $m = 1, \ldots, M_l$, and $l = 1, \ldots, L$. Based on the choice of degree Q, the length of subpulse M_l, and total number of subpulses L, every subpulse can have a unique property varying from a chirp-like sequence on one end to noise-like sequences on the other end.

The conventional MF response of the received signal with the reference signal is given as

$$\bar{r}_k = \sum_{n=-N+k}^{N-k} x_n y_{n+k}^*, \tag{2}$$

where $k \in \{1-N, \ldots, N-1\}$. In the case of subpulse processing, the pulse compression operation consists of performing L matched filtering operations, one for each subpulse. Let $\mathbf{0}_l$ be a vector of zeros as $\mathbf{0}_l = [0_1, 0_2 \cdots, 0_{M_l}]^T$ and

$$\mathbf{U} = \begin{bmatrix} \widetilde{\mathbf{x}}_1 & \mathbf{0}_1 & \ldots & \mathbf{0}_1 \\ \mathbf{0}_2 & \widetilde{\mathbf{x}}_2 & & \vdots \\ \vdots & \vdots & \ddots & \\ \mathbf{0}_L & \ldots & & \widetilde{\mathbf{x}}_L \end{bmatrix} \in \mathbb{C}^{N \times L}. \tag{3}$$

Let $\mathbf{u}_l = [\mathbf{0}_1, \ldots, \mathbf{u}_l, \ldots, \mathbf{0}_L]^T \in \mathbb{C}^N$ be the l^{th} column of $\mathbf{U}$, $l = 1, \ldots, L$. Thus, the l^{th} MF operation for each of the zero-padded subpulse reference signal is represented as

$$(\mathbf{y} \circledast \mathbf{u}_l)_k = \sum_{n=-N+k}^{N-k} y_n u_{n+k}^*, k \in \{1-N, \cdots, N-1\}. \tag{4}$$

Finally, the combined result of l matched filters is represented as $\bar{r}_k = \sum_{l=1}^{L} (\mathbf{y} \circledast \mathbf{u}_l)_k, k \in \{1-N, \cdots, N-1\}$, and is equivalent to the conventional MF operation mentioned in (2). However, to decrease the MF loss in the received side, the subpulses are non-coherently integrated as

$$\sum_{l=1}^{L} |(\mathbf{y} \circledast \mathbf{u}_l)_k| = \hat{r}_k, \ k \in \{1-N, \cdots, N-1\}. \tag{5}$$

[1]The fast-time Doppler shift may be ignored in most radar applications, and the Doppler shift appears only in the slow time. This phenomena, however, is of particular importance in this work.

[2]Doppler tolerance property arises in a sequence when its unwrap phase varies in a quadratic manner (i.e. Q = 2). As this is being handled directly in the objective function, the resultant sequence is bound to have better performance for moving targets [7].

This operation (subpulse Doppler processing) in (5) provides a better MF gain in the presence of large Doppler shifts than the coherent integration in (4). Note that the additional step in the processing adds a new dimension to the analysis. Besides the fast and slow-time domains, the subpulse dimension, denoted by k, can be jointly evaluated in order to improve the Doppler estimation performance.

III. Proposed Method

The optimization problem mentioned in (1) is hard to solve since each r_k is quadratically related to $\{x_n\}_{n=1}^N$ and each $\{x_n\}_{n=1}^N$ is non-linearly related to $a_{\{q,l\}}$. In [15], minimization of the aforementioned quartic objective function in (1), is shown to be "almost equivalent" to minimization of the following quadratic function,

$$\underset{\{x_n\}_{n=1}^N;\{\chi_g\}_{g=1}^{2N}}{\text{minimize}} \sum_{g=1}^{2N} \left| \sum_{n=1}^{N} x_n e^{-j\omega_g n} - \sqrt{N} e^{j\chi_g} \right|^2 \tag{6}$$

s.t. w_g are the Fourier frequencies: $w_g = \frac{2\pi}{2N} g$ and $\chi_g \in [0, 2\pi]$, where $g = 1, \ldots, 2N$. The above equation can be further simplified and written in a more compact form as (to within a multiplicative constant)

$$||\boldsymbol{A}^H \bar{\mathbf{x}} - \mathbf{v}||^2 \tag{7}$$

where $\boldsymbol{\alpha}_g^H = [e^{-j\omega_g}, \cdots, e^{-j2N\omega_g}]$ and $\boldsymbol{A}^H$ is the unitary $2N \times 2N$ Discrete Fourier Transform (DFT) matrix

$$\boldsymbol{A}^H = \frac{1}{\sqrt{2N}} [\boldsymbol{\alpha}_1^H, \cdots, \boldsymbol{\alpha}_{2N}^H]^T, \tag{8}$$

$\bar{\mathbf{x}}$ is the sequence $\{x_n\}_{n=1}^N$ padded with N zeros, i.e. $\bar{\mathbf{x}} = [x_1, \cdots, x_N, 0, \cdots, 0]_{2N\times 1}^T$ and $\mathbf{v} = \frac{1}{\sqrt{2}}[e^{j\chi_1}, \cdots, e^{j\chi_{2N}}]^T$. For given $\{x_n\}$, CAN [15] minimizes (7) by alternating the optimization between $\bar{\mathbf{x}}$ and $\mathbf{v}$. Let $\bar{\mathbf{x}}^{(i)} = [x_1^{(i)}, \cdots, x_N^{(i)}, 0, \cdots, 0]_{2N\times 1}^T$ represent the value of $\mathbf{x}$ at iteration i. Similarly, let D_i represent the value of $||\boldsymbol{A}^H \bar{\mathbf{x}}^{(i)} - \mathbf{v}^{(i)}||_2^2$ at iteration i. Then we have $D_{i-1} \geq D_i$. Further in the i^{th} iteration, the objective can be rewritten as

$$||\mathbf{s} - \boldsymbol{\beta}||_2^2 \tag{9}$$

where $\mathbf{s} = \boldsymbol{A}^H \bar{\mathbf{x}}^{(i)}, \mathbf{d} = \boldsymbol{A}\mathbf{v}^{(i)}$, $\boldsymbol{\beta} = \mathbf{v}^{(i)}$, $y_n = e^{j \arg(d_n)}$, and $\chi_g = \arg(s_g)$.

Now, let us define, $\boldsymbol{\rho} = |\mathbf{y}|$ and $\boldsymbol{\psi} = \arg(\mathbf{y})$, where ρ_n and ψ_n, $n = 1, \ldots, N$, are the magnitude and phase of every entry of $\mathbf{y}$, respectively. By considering the polynomial phase and unimodular constraints of Problem $\mathcal{P}_1$ into the objective function, (9) can be rewritten as [7], $\sum_{l=1}^{L} \sum_{m=1}^{M_l} \left| e^{j(\sum_{q=0}^{Q} a_{\{q,l\}} m^q)} - \rho_m e^{j\psi_m} \right|^2$, where $m = 1, \ldots, M_l$, and $l = 1, \ldots, L$.

Since the objective in (9) is separable in the sequence variables, minimization problem can now be split into L sub-problems (each of which can be solved in parallel). For ease of notation, let us assume that the polynomial phase coefficients and sub-sequence length of the l-th subpulse, say $a_{\{q,l\}}$ and M_l are indicated as $\widetilde{a}_q$ and $\widetilde{M}$ respectively, where $\widetilde{M} \in [M_1, \cdots, M_L]$. Thus, dropping the subscript-l, each of the sub-problem can be further defined as

$$\mathcal{P}_2 \left\{ \underset{\widetilde{a}_q}{\text{minimize}} \quad \sum_{m=1}^{\widetilde{M}} \left| e^{j(\sum_{q=0}^{Q} \widetilde{a}_q m^q)} - \rho_m e^{j\psi_m} \right|^2, \right. \tag{10}$$

where we have considered the unimodular and polynomial phase constraints of Problem $\mathcal{P}_1$ directly in the definition of the code entries in Problem $\mathcal{P}_2$. Further, using Majorization-Minimization (MM) framework (10) can be written as [7],

$$\mathcal{P}_3 \left\{ \underset{\widetilde{a}_q}{\text{minimize}} \quad \sum_{m=1}^{\widetilde{M}} \left[\rho_m \cos(\theta_m^{(i)}) \left(\sum_{q=0}^{Q} \widetilde{a}_q m^q \right) - \widetilde{b}_m \right]^2, \right. \tag{11}$$

where $\theta_m = \sum_{q=0}^{Q} \widetilde{a}_q m^q - \psi_m$, $\widetilde{b}_m = \rho_m \cos(\theta_m^{(i)}) \left(\psi_m + \theta_m^{(i)} \right) - \rho_m \sin(\theta_m^{(i)})$. Now, considering a generic sub-sequence index l, we define $\boldsymbol{\eta} = [1, 2, 3, \cdots, \widetilde{M}]^T \in \mathbb{Z}_+^{\widetilde{M}}$, $\boldsymbol{\eta}^q$ implying each element of $\boldsymbol{\eta}$ is raised to the power of q, $q = 0, 1, \ldots, Q$. Further,

$$\begin{aligned} \boldsymbol{\gamma} &= \rho_m \cos(\theta_m^{(i)}) \odot [1, \cdots, 1]^T \in \mathbb{R}^{\widetilde{M}}, \\ \widetilde{\boldsymbol{A}} &= \text{Diag}\,(\boldsymbol{\gamma})[\boldsymbol{\eta}^0, \boldsymbol{\eta}^1, \cdots, \boldsymbol{\eta}^Q] \in \mathbb{R}^{\widetilde{M}\times Q+1}, \\ \mathbf{z} &= [\widetilde{a}_0, \widetilde{a}_1, \cdots, \widetilde{a}_Q]^T \in \mathbb{R}^{Q+1}, \\ \widetilde{\mathbf{b}} &= [\widetilde{b}_1, \widetilde{b}_2, \cdots, \widetilde{b}_{\widetilde{M}}]^T \in \mathbb{R}^{\widetilde{M}}, \end{aligned} \tag{12}$$

the optimization problem in (11) can be rewritten as

$$\left\{ \underset{\mathbf{z}}{\text{minimize}} \quad ||\widetilde{\boldsymbol{A}}\mathbf{z} - \widetilde{\mathbf{b}}||_2^2, \right. \tag{13}$$

which is the standard Least Squares (LS) problem. As a result, the optimal $\mathbf{z}^\star = \widetilde{\boldsymbol{A}}^{(\dagger)} \widetilde{\mathbf{b}} = [\widetilde{a}_0^\star, \widetilde{a}_1^\star, \cdots, \widetilde{a}_Q^\star]^T$ would be calculated and the optimal sequence will be synthesized.

Using the aforementioned setup for a generic sub-sequence index l, we calculate all the $\widetilde{\mathbf{x}}_l$s pertaining to different sub-sequences and derive $\{x_n\}_{n=1}^N$ by concatenating all the $\widetilde{\mathbf{x}}_l$s. The algorithm successively improves the objective and an optimal value of $\mathbf{x}$ is achieved. The details of the implementation which includes the sequence generation and non-coherent subpulse integration can be found in Algorithm 1.

IV. Results

In this section, we will assess the performance of the proposed algorithm and then discuss its application. Using a case study with reference to the work [5], we highlight the improvement achievable with the proposed algorithm.

A. Algorithm Performance Analysis

Fig. 2a shows the unwrap phase plot of the optimal sequence (multi-colored) compared with the seed sequence (black). As evident from the plot, every subpulse possesses a quadratic phase behavior which imparts the waveform its Doppler-tolerant property. The sidelobe reduction is achieved (shown in Fig. 2b) while retaining the quadratic phase constraint within every subpulse. Fig. 2c proves the Doppler tolerance property of the code sequence. The design parameters considered for running the Algorithm 1 are: $N = 500$, $M = 10$ and $L = 50$. The Algorithm 1 is fast and requires a few iterations to

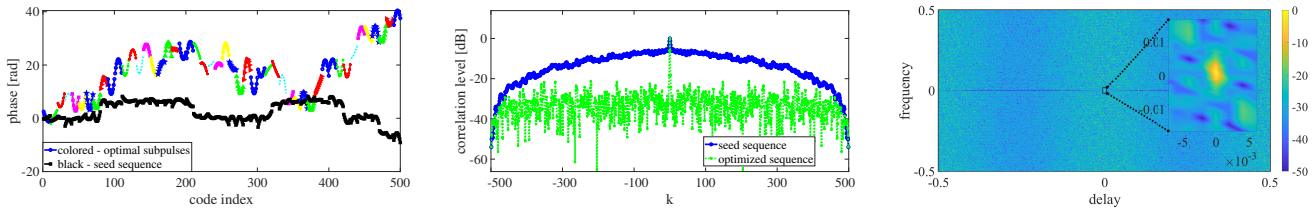

(a) Unwrap phase for different subpulses (b) sidelobe minimization (c) Ambiguity function

Fig. 2: Unwrapped phase value, autocorrelation and Doppler tolerant ambiguity function plots for optimal code sequence

Algorithm 1 Subpulse processing using optimal sequence with minimum ISL and Doppler tolerance property

Require: N, L and $\widetilde{M}$
Ensure: $\mathbf{x}^{(i)}$
Waveform Design
Set $i = 0$, initialize $\mathbf{x}^{(0)}$.
while Stopping criterion is not met **do**
  Obtain $\mathbf{s}$, v_g, $\mathbf{d}$, $y_n^{(i+1)}$, $\boldsymbol{\psi}$, and $\boldsymbol{\rho}$
  for $l \leftarrow 1$ *to* L **do**
    Obtain $\widetilde{\boldsymbol{\psi}}_l$, $\widetilde{\boldsymbol{\rho}}_l$, $\theta_m^{(i)}$, and $\widetilde{b}_m$
    Obtain $\boldsymbol{\eta}$, $\boldsymbol{\gamma}$, $\widetilde{\boldsymbol{A}}$, $\mathbf{z}$, and $\widetilde{\mathbf{b}}$ from (12)
    $\mathbf{z}^\star = \widetilde{\boldsymbol{A}}^{(\dagger)}\widetilde{\mathbf{b}}$
    $\widetilde{\mathbf{x}}_l = e^{(j(\widetilde{\boldsymbol{A}}\mathbf{z}^\star))}$
  $\mathbf{x}^{(i+1)} = [\widetilde{\mathbf{x}}_1^T, \widetilde{\mathbf{x}}_2^T, \cdots, \widetilde{\mathbf{x}}_L^T]^T \in \mathbb{C}^N$
Receiver Design
$\mathbf{s} = \mathbf{x}^{(i+1)}$
for $l \leftarrow 1$ *to* L **do**
  $\boldsymbol{\gamma}_l = |(\mathbf{s} \circledast \mathbf{u}_l)_k|$, $\in \mathbb{C}^{2N-1}$ and $k = 1-N, \cdots, N-1$
$\hat{\mathbf{r}} = \sum_{l=1}^{L} \boldsymbol{\gamma}_l$
return

converge[3]. Further, the next section discusses its applications and puts forth its advantages over existing techniques.

B. Case Study

We discuss its application in Noise surveillance radars and Automotive radars in the following subsections.

1) Application 1 - Noise Radar Systems: In this section, a performance analysis is presented for a setup in which the waveform and target properties of Noise radar are operating frequency (f_c) is 3GHz, wavelength (λ) is 0.1m, pulse width (T_c) is 125μs, chip width (τ) is 50ns, bandwidth (B) is 20MHz, sequence length (N) is 2500, target speed, v is 680m/s - 2040m/s (Mach2 - Mach6), Doppler frequency (f_d) is 13.60 - 40.80kHz, and parameter ζ is 1.7 - 5.1 cycles. We compare the MF response of optimized code subpulse waveform with frequency-modulated noise signals (FM Noise) using subpulse processing architecture [5]. As a reference, the performance of a complex random sequence using conventional MF and subpulse processing method is provided. Here, the entries of the complex random sequence $\mathbf{x} = [x_1, x_2, \ldots, x_N]^T$ is defined as $x_n = e^{j\phi_n}$, $\phi_n = 2\pi z$, $n \in 1, \cdots, N$, where z is drawn from a Gaussian distribution with zero mean and unit variance. The FM Noise waveform is composed of 4 subpulses each of length 31.25μs. Further, the number of Doppler tolerant subpulses in optimized code waveform, L incorporated in the overall code sequence was set to 25 where the subpulse length $\widetilde{M}$ is 100 elements long of 5μs each. The subpulse length for the optimized code is calculated such that one quarter of a Doppler cycle (i.e. ζ) is covered in it. Thus, the subpulse length is decreased from 31.25μs in FM Noise waveform to 5μs in optimized code subpulse waveform, allowing the subpulse processing technique to achieve optimal result. Fig.3 shows an improvement of $\sim$ 14dB in the MF response of the optimized code subpulse waveform as compared to FM Noise using subpulse processing method. The conventional MF response of a complex random sequence shows poor performance as expected from its lack of Doppler tolerance. When the random sequence is processed using subpulse processing method with the same subpulse length as of the FM Noise waveform, its peak correlation value matches with the FM Noise waveform (refer magnified plot in Fig.3).

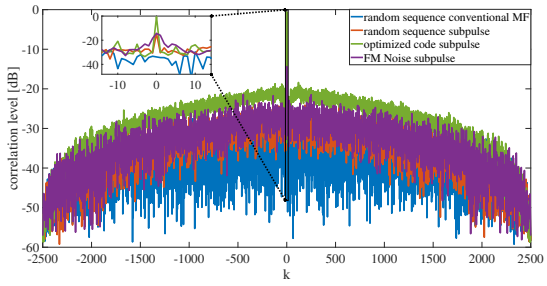

Fig. 3: Improvement in the cumulative matched filter gain from Subpulse processing method

2) Application 2 - Automotive Radar Sensors: In this section, we discuss another application where the target speeds are relatively low (i.e. maximum relative velocity of 420kmph/120m/s) and the pulse widths are less than 90μs. The specifications of a typical commercial-off-the-shelf (COTS) radar sensor for long range sensing application are operating frequency (f_c), wavelength (λ), and bandwidth (B) as 76.5GHz, 0.0039m, and 150MHz respectively. For a target with a maximum relative speed of 120m/s (i.e. 420kmph), the Doppler frequency (f_d) of 27.20kHz is observed at the sensor. The parameter ζ is 3.4 cycles due to this Doppler frequency and pulse width time is (60μs). The Doppler tolerant property of LFM waveform used in FMCW radars helps in retaining the gain of the MF in the presence of longer pulses for dynamic target detection. Although these waveforms perform well in this respect, their interference immunity from a statistical

[3]for more details on the performance of Algorithm 1, refer [7].

analysis standpoint is low, as explained in [7]. Thus, PMCW radars with unique phase in every subpulse provide less cross-correlation and better interference immunity. In addition, Doppler tolerant behavior (quadratic phase) in every subpulse can provide better MF gain. As a result, the flexibility of waveform design in phase and time domain in the PMCW radars, allows a greater degree of freedom in addressing the whole problem of interference.

Using the proposed algorithm, we design a code of length 9000 for a PMCW waveform with a pulse width of 60μs, 15 subpulses of length 4μs each, and quadratic phase behavior (i.e. $Q = 2$). The sampling frequency is set to 150MHz and therefore the chip time is 6.66ns. With this setup, the MF performance of the PMCW waveform suitably matches the performance of FMCW waveform with an added advantage of interference immunity. Further, the statistical interference analysis is performed using the following waveform types: random sequence, LFM waveform in FMCW radars (for similar-slope and sweeping slope type interference) and code sequences designed using the proposed algorithm. The procedure of this statistical experiment is as follows:

1) Consider two sequences from a selected category of signals (say $\mathbf{x} = [x_1, \cdots, x_N]^T$ and $\mathbf{y} = [y_1, \cdots, y_N]^T \in \mathbb{C}^N$, $N > 0$).
2) Compute the linear aperiodic cross-correlation of these signals, and find $\bar{c}_k = \sum_{n=1}^{N} x_n y^*_{n+k}$, such that $k = -(N-1), \ldots, 0, \ldots, N-1$. Here, we use the convention that $x_n = 0$ and $y_n = 0$ when $n \notin \{1, \cdots, N\}$.
3) Calculate $\bar{c}_{max} = \max(|c_k|)$.
4) Let $\xi = 20\log_{10}(\frac{\bar{c}_{max}}{N})$.
5) Record the value (i.e. ξ) for the current trial and repeat the experiment until the desired number of trials.

Note that ξ which is a stochastic value will be calculated for different categories of waveforms that are mentioned above. In case the sequences $\mathbf{x}$ and $\mathbf{y}$ are similar, ξ is approximately zero, since both the sequences are fully correlated. In the case of partially correlated waveforms, ξ is negative, and as the correlation between the waveforms decreases, ξ decreases further. TABLE I presents the excerpts of the analysis.

TABLE I: Statistical interference comparative analysis

Waveform type	**max. cross-correlation ξ (μ, σ)**	**mean occurrence probability**
Random sequence	-14.1dB, 3dB	0.1
FMCW - similar slope [16]	-0.2dB, 0.1dB	0.3
FMCW - sweeping slope	-1.5dB, 1.4dB	0.1
Proposed sequence	-14.1dB, 3dB	0.1

In general, random sequences have the lowest mean value of ξ. Interestingly, the mean value and distribution of ξ generated using the proposed sequence exhibits a large overlap with the distribution of ξ generated using complex unimodular random phase sequences (refer TABLE I). When compared to the categories where conventional FMCW waveforms are employed, utilizing the proposed approach resulted in an overall decreased cross-correlation of 12dB. As a result, the proposed technique shows improved interference immunity as compared to the state of the art techniques.

V. Conclusion

A joint waveform and receiver design approach is presented to synthesize interference immune and Doppler tolerant waveforms which can be used with subpulse processing technique to achieve optimal performance. The proposed algorithm is stable and requires few iterations to synthesize the waveform. Its application to surveillance and automotive radars was discussed and the algorithm performance is compared to the existing approach in the literature for validation.

References

[1] S. Alland, W. Stark, M. Ali, and M. Hegde, "Interference in automotive radar systems: Characteristics, mitigation techniques, and current and future research," *IEEE Signal Processing Magazine*, vol. 36, no. 5, pp. 45–59, 2019.

[2] C. Aydogdu, M. F. Keskin, G. K. Carvajal, O. Eriksson, H. Hellsten, H. Herbertsson, E. Nilsson, M. Rydstrom, K. Vanas, and H. Wymeersch, "Radar interference mitigation for automated driving: Exploring proactive strategies," *IEEE Signal Processing Magazine*, vol. 37, no. 4, pp. 72–84, 2020.

[3] M. A. Richards, J. Scheer, W. A. Holm, and W. L. Melvin, *Principles of modern radar*. Citeseer, 2010.

[4] T. Thayaparan, M. Daković, and L. Stanković, "Mutual interference and low probability of interception capabilities of noise radar," *IET Radar, Sonar & Navigation*, vol. 2, pp. 294–305(11), August 2008.

[5] G. Beltrão, L. Pralon, A. Barreto, M. Alaee-Kerahroodi, and M. R. B. Shankar, "Subpulse processing for unambiguous doppler estimation in pulse-doppler noise radars," *IEEE Transactions on Aerospace and Electronic Systems*, vol. 57, no. 6, pp. 3813–3826, 2021.

[6] G. Beltrao, L. Pralon, M. Menezes, P. Vyplavin, B. Pompeo, and M. Pralon, "Subpulse processing for long range surveillance noise radars," in *International Conference on Radar Systems (Radar 2017)*, 2017, pp. 1–4.

[7] R. Amar, M. Alaee-Kerahroodi, P. Babu, and B. Shankar M.R., "Designing interference-immune doppler-tolerant waveforms for radar systems," *IEEE Transactions on Aerospace and Electronic Systems*, pp. 1–20, 2022.

[8] I. A. Arriaga-Trejo, "Design of constant modulus sequences with doppler shift tolerance and good complete second order statistics," in *2020 IEEE International Radar Conference (RADAR)*, 2020, pp. 274–279.

[9] X. Feng, Q. Song, Z. Zhang, and Y. Zhao, "Novel waveform design with low probability of intercept and high doppler tolerance for modern cognitive radar," in *2019 IEEE International Conference on Signal, Information and Data Processing (ICSIDP)*, 2019, pp. 1–6.

[10] Z.-J. Wu, Z.-Q. Zhou, C.-X. Wang, Y.-C. Li, and Z.-F. Zhao, "Doppler resilient complementary waveform design for active sensing," *IEEE Sensors Journal*, vol. 20, no. 17, pp. 9963–9976, 2020.

[11] M. Alaee-Kerahroodi, S. Sedighi, B. Shankar M.R., and B. Ottersten, "Designing (in)finite-alphabet sequences via shaping the radar ambiguity function," in *ICASSP 2019 - 2019 IEEE International Conference on Acoustics, Speech and Signal Processing (ICASSP)*, 2019, pp. 4295–4299.

[12] A. Aubry, A. De Maio, B. Jiang, and S. Zhang, "Ambiguity function shaping for cognitive radar via complex quartic optimization," *IEEE Transactions on Signal Processing*, vol. 61, no. 22, pp. 5603–5619, 2013.

[13] G. Cui, Y. Fu, X. Yu, and J. Li, "Local ambiguity function shaping via unimodular sequence design," *IEEE Signal Processing Letters*, vol. 24, no. 7, pp. 977–981, 2017.

[14] M. E. Levanon Nadav, *Radar Signals*. John Wiley & Sons, Inc., Publication, 2004.

[15] P. Stoica, H. He, and J. Li, "New algorithms for designing unimodular sequences with good correlation properties," *IEEE Transactions on Signal Processing*, vol. 57, no. 4, pp. 1415–1425, 2009.

[16] R. Amar, M. Alaee-Kerahroodi, and M. R. Bhavani Shankar, "Fmcw-fmcw interference analysis in mm-wave radars; an indoor case study and validation by measurements," in *2021 21st International Radar Symposium (IRS)*, 2021, pp. 1–11.